Korean J. Chem. Eng., **28**(8), 1773-1778 (2011)
DOI: 10.1007/s11814-011-0004-x

Performance of fluidized bed electrode in a molten carbonate fuel cell anode

Jubing Zhang, Zhaoping Zhong†, Jianmin Xiao, Zongming Fu, Jinxiao Zhao, Weiling Li, and Min Yang

School of Energy and Environment, Southeast University, Nanjing 210096, China
(*Received 29 June 2010 • accepted 3 January 2011*)

Abstract−A fluidized bed electrode could lower concentration polarization and activation polarization because of its high mass and heat transfer coefficient. The polarization characteristics of the fluidized bed electrode are systematically investigated in a molten carbonate fuel cell anode with an O_2/CO_2/gold reference electrode. The results show that polarization performance of the anode is improved by selecting proper flow rates of H_2, O_2 and CO_2, choosing suitable nickel particle content together with appropriate O_2/CO_2 ratio, and increasing reaction temperature as well as the area of the current collector. Limiting current density of 115.56 $mA \cdot cm^{-2}$ is achieved under optimum performance as follows: a cylindrically curved nickel plate current collector, nickel particle content of 7.89%, the reaction temperature of 923 K, H_2 flow rate of 275 $mL \cdot min^{-1}$, O_2/CO_2 flow rate of 10/20 $mL \cdot min^{-1}$ and O_2/CO_2 ratio of 1 : 2.

Key words: Fluidized Bed Electrode, Molten Carbonate Fuel Cell, Anode, Polarization, Current Density

INTRODUCTION

The electrode used in a molten carbonate fuel cell (MCFC) [1-5] is a porous gas-diffusion electrode which is in the shape of a plate and separated by a ceramic matrix containing electrolyte [6-8]. It is mainly accepted that the electrochemical reaction of an anode only occurs at gas-liquid-solid boundaries due to the low solubility and mass transfer coefficient of gas reactant [8-11]. Therefore, a MCFC electrode must be porous so it can provide many active reaction sites for anode reactions. Meanwhile, electrode electronic conductivity is also emphasized for the flow of electrons to and from the reaction sites. In addition, it is difficult to replace the electrode because of its special structure [9,12]. These requirements increase the expense and difficulty of electrode manufacture. When used in MCFC, the fluidized bed electrode could overcome all these disadvantages mentioned above.

Fluidization [8-14] is a technique whereby fine solids are contacted with fluid to transform into a fluid-like state for the purpose of mass or heat transfer between the phases with or without simultaneous chemical reaction. Extensive work has been reported on fluidized bed electrodes in industrial applications. Yen and Yao [12] reviewed the application of fluidized bed electrodes in metal recovery from dilute copper solutions and found that fin-type current feeders provided higher deposition rates for the same electrode potential than planar current feeders in fluidized bed electrodes. Vatistas and Bartolozzi [13] introduced a three-dimensional current feeder for fluidized bed electrodes to improve the current distribution in the bed and to reduce the maldistribution of potential. Yap and Mohamed [14] presented a galvanic static batch system with various cathode materials coupled with zinc which was designed for the recovery of gold from cyanide solutions. Kusakabe et al. [15] studied the charge transfer rate in copper deposition from acidic aqueous solutions containing copper ion for liquid-solid and gas-liquid-solid fluidized bed electrode systems.

For a three-phase fluidized bed electrode, the introduction of gas flow into the bed provides the following advantages. First, the gas flow enhances mass transfer in the bed [16]. Higher mass transfer facilitates transfer of ionic species to and from the fluidized particles, which leads to fairly good performance of the fuel cell due to the reduction of concentration polarization losses. Moreover, the gas flow also enhances heat transfer in the bed. There hardly exists a temperature gradient in a fluidized bed due to higher heat transfer coefficient, which facilitates the electrochemical reaction. In addition, its construction and replacement is especially easy in contrast to a porous gas-diffusion electrode in MCFC. The commercial use of a fluidized bed electrode instead of porous gas-diffusion electrode in conventional MCFC would be a great breakthrough.

So far, some studies have been reported on applying the fluidized bed electrode into fuel cells. Matsuno et al. [8-11] applied the fluidized bed electrode into a MCFC anode and alkaline fuel cell cathode. Li et al. [17] combined the fluidized bed electrode with solid oxide fuel cell while replacing carbon fuel with gas fuel and found that undesirable high ohmic impedance of electrolyte was primarily responsible for the poor performance of carbon fuel. Berent et al. [18] studied the anodic and cathodic electrode of a fluidized bed electrode fuel cell and observed that polarization performance decreased in the cathode while increasing in the anode with the increase in fluidization.

In this study, a fluidized bed electrode fuel cell (FEBFC) anode is designed based on the studies of Matsuno et al. The influences of H_2 flow rate, O_2/CO_2 flow rate, reaction temperature, nickel particle content, current collector type and the O_2/CO_2 ratio on polarization characteristics of anode are systematically investigated.

EXPERIMENTS

1. Materials

Potassium carbonate, lithium carbonate and nickel particles came from Sinopharm Chemical Reagent Co., Ltd., Xinjiang Westar Bio-

†To whom correspondence should be addressed.
E-mail: zzhong@seu.edu.cn

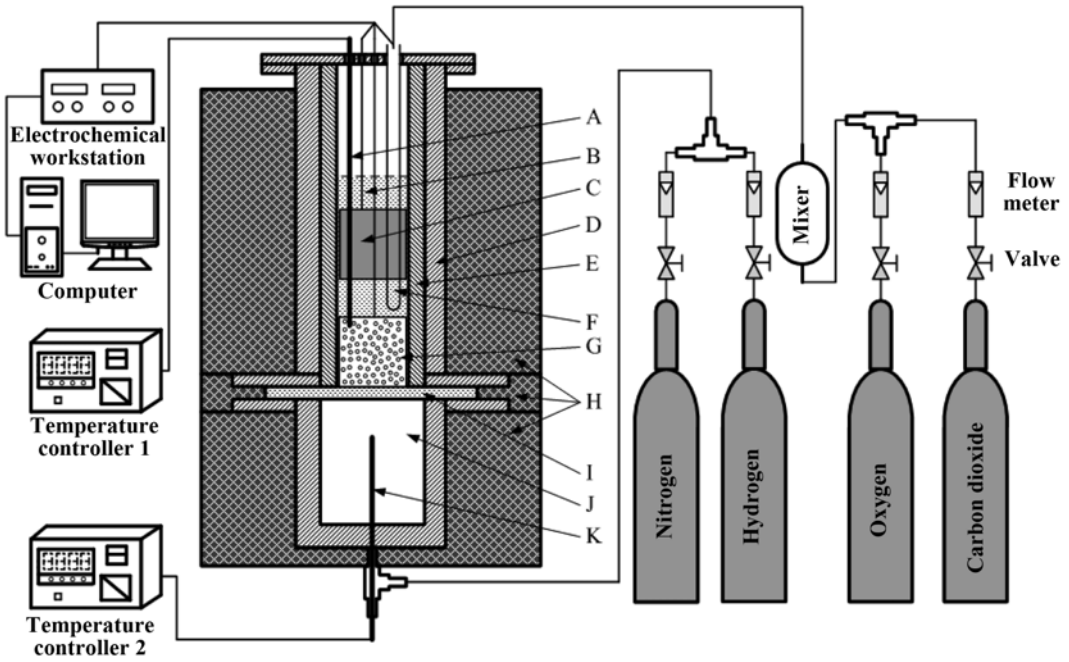

Fig. 1. Diagram of experimental apparatus.

A. Thermocouple 1 D. 316L stainless steel tube G. Nickel grain J. Gas preheater
B. Molten carbonate E. Alumina tube H. Electric furnace K. Thermocouple 2
C. Counter electrode F. Reference electrode I. Gas distributor

engineering Co., Ltd., (Shanghai Office) and Shenzhen XinLiLai Industrial Materials Co., Ltd., respectively.

H_2, N_2, O_2 and CO_2 (99.99% for all) came from Jiangsu Topgrand Petrifaction Industry Gas Co. Ltd.

2. Test of Polarization Characteristic

Polarization curves derived from a CS150 electrochemical workstation are used to estimate the polarization characteristics of the self-built FEBFC anode (Fig. 1). The anode mainly consists of a SUS-316L outer shell, an inner corundum tube, a gas distributor, a counter electrode, a current collector, a reference electrode, nickel particles and a gas preheater. The inner corundum tube is 520 mm in height with external diameter of 45 mm and inside diameter of 35 mm. A SUS-316L 840 mesh powder sintered plate is used as the gas distributor with 45 mm in diameter and 8 mm in thickness. The reference electrode is a closed-end corundum tube (external diameter of 8 mm and length of 550 mm) with a gold wire (0.6 mm in diameter) inside. There is a 1 mm hole at the bottom of the corundum tube to realize carbonate ion transfer. The corundum tube is sheathed by the other closed-end corundum tube (external diameter of 12 mm, inside diameter of 10 mm and length of 60 mm) to minimize contamination of the reference molten carbonate by anode gas. The two closed-end corundum tubes in reference electrode are connected with high temperature inorganic adhesive. The reference electrode is in equilibrium with the gas mixture (with different O_2/CO_2 ratios) which is fed through an inner corundum tube at different gas flow rates (Fig. 2). Fig. 3 shows the two different types of current collectors used in this study. One is a flat nickel plate (50×32×0.4 mm), while the other is a cylindrically curved nickel plate (50×120×0.4 mm). The counter electrode has the same dimensions as the cylindrically curved nickel plate current collector. Both the current collector and the counter electrode are connected to alumina-

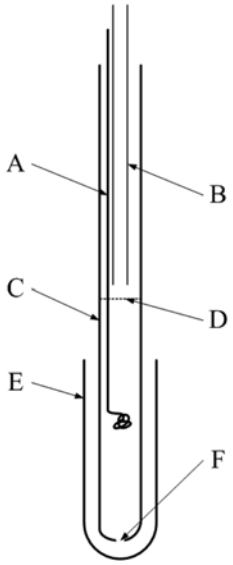

Fig. 2. Diagram of reference electrode.

A. Gold wire D. Melt lever
B. Inlet tube E. Closed-end alumina tube
C. Closed-end alumina tube F. 1 mm hole

sheathed nickel wires of 2 mm in diameter. Prior to all the experiments, the current collector and counter electrode are polished with sandpaper and rinsed in distilled water. The electrolyte used here is a mixture of 62 mol% Li_2CO_3 and 38 mol% K_2CO_3 with the total weight of 350 g.

Two electric furnaces are used to heat the half cell, and each of them is kept at constant temperature by an independent temperature controller. Both the temperatures are measured by thermocouple,

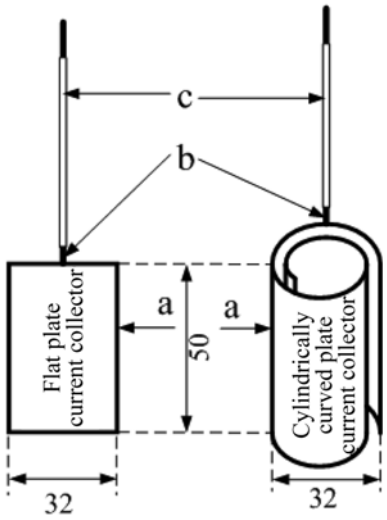

Fig. 3. Diagram of current collector.
a. Nickel plate b. Nickel wire c. Alumina tube

while the thermocouple related to the upper electric furnace should be protected by alumina sheath due to the causticity of electrolyte. The fluidizing gas (N_2) is heated by gas preheater before being fed into the anode through the gas distributor.

Initially, the FBEFC anode was heated to 873 K with the electric furnace, and then a mixture of carbonate and nickel particles was added into the anode. Subsequently, the reference electrode, counter electrode and current collector were put inside in turn when the anode reached the expected temperature. After that, the cover was closed and the inlet pipe of the reference electrode was laid correctly. Finally, the circuit connection could be complete to start the test of polarization performance of the FBEFC anode. A certain N_2 flow was supplied to keep the inert atmosphere in anode during the heating process, which was also beneficial to avoid leakage of carbonate from air distributor to gas preheater. When the experiment started, N_2 had to be switched to H_2.

RESULTS AND DISCUSSION

When current passes through an electrode, the electrode potential departs from equilibrium electrode potential. The difference between them is called polarization, quantified in terms of an overpotential (η) as in the equation.

$$\eta = E - E^0 \quad (1)$$

Where, E stands for electrode potential with current, while E^0 stands for equilibrium electrode potential.

Using H_2 as fuel, the electrochemical reaction at working electrode takes place as follows:

$$H_2 + CO_3^{2-} = H_2O + CO_2 + 2e^- \quad (2)$$

In this research, H_2 flow rate, reaction temperature, O_2/CO_2 flow rate, nickel particle content, current collector type and O_2/CO_2 ratio are considered as main influence factors. The experimental conditions are illustrated in Table 1.

1. The Influence of H_2 Flow Rate

H_2 is not only a reactant for anode reaction, but also a fluidization medium for the fluidized bed. Thus, the H_2 flow rate should affect polarization performance enormously. Fig. 4 shows how it affects the polarization curve of the anode without nickel particles in the anode.

With different H_2 flow rates of 75, 140 and 275 mL·min^{-1} separately, limiting current density of anode is 47.8, 58, and 66 mA·cm^{-2} accordingly. Current density under the same overpotential also shows an increase as the H_2 flow rate rises. However, no limiting current at the experimental range could be observed when the H_2 flow rate was 385 mL·min^{-1}. As the flow rate increases, the turbulence and

Table 1. Experimental conditions

No.	Particle content/ %	Flow rate/ mL·min^{-1}		Reaction temperature/ K	Current collector	O_2/CO_2 ratio
		H_2	O_2/CO_2			
1	0	75	10/20	923	a	1 : 2
2	0	140	10/20	923	a	1 : 2
3	0	275	10/20	923	a	1 : 2
4	0	385	10/20	923	a	1 : 2
5	7.89	75	10/20	923	a	1 : 2
6	7.89	140	10/20	923	a	1 : 2
7	7.89	275	10/20	923	a	1 : 2
8	7.89	385	10/20	923	a	1 : 2
9	4.11	275	10/20	923	a	1 : 2
10	11.39	275	10/20	923	a	1 : 2
11	7.89	275	5/10	923	a	1 : 2
12	7.89	275	15/30	923	a	1 : 2
13	7.89	275	10/20	873	a	1 : 2
14	7.89	275	10/20	898	a	1 : 2
15	7.89	275	10/20	948	a	1 : 2
16	7.89	275	10/20	923	b	1 : 2
17	7.89	275	10/20	923	a	1 : 3
18	7.89	275	10/20	923	a	1 : 1

[a]Cylindrically curved plate current collector
[b]Flat plate current collector

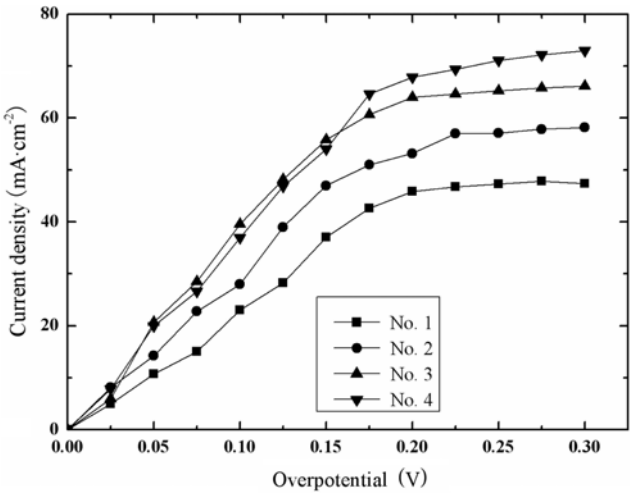

Fig. 4. Polarization curves for anode under different H_2 flows without nickel particles.

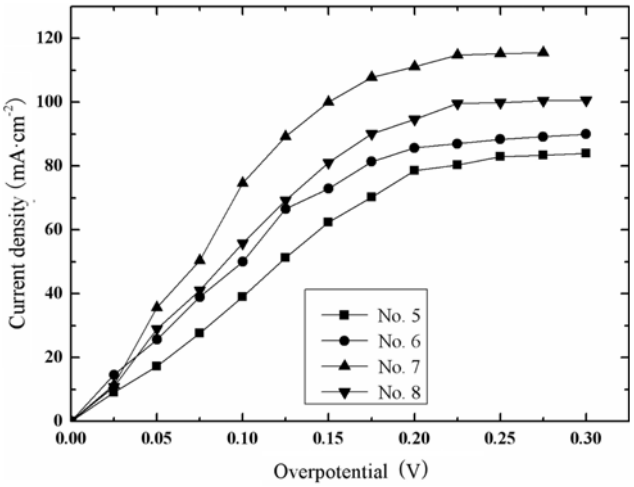

Fig. 5. Polarization curves for anode under different H_2 flows with nickel particle content of 7.89%.

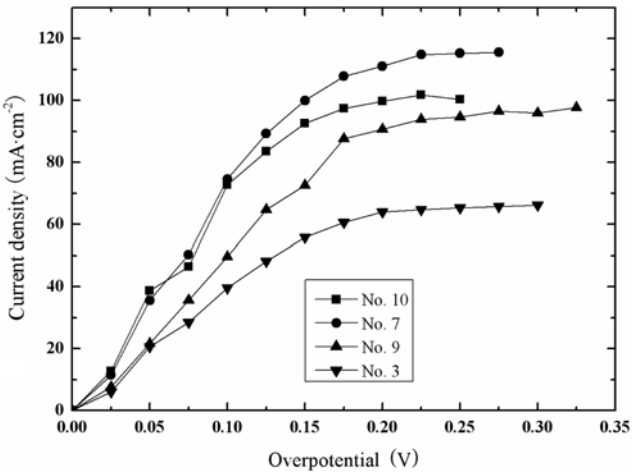

Fig. 6. Polarization curves for anode with different nickel particle content.

mass transfer in the anode are strengthened, which lowers concentration polarization. The concentration polarization here is mainly caused by depletion of reactant (H_2) as well as by accumulation of product (vapor and CO_2) on the electrode surface. Therefore, an increase is observed in limiting current density as well as current density under the same overpotential accompanied with the increase of H_2 flow rate. When H_2 flow rate increases from 275 to 385 mL·min^{-1}, polarization performance is also promoted, but the effect is not as obvious as that under low flow rate. It is probably because H_2 flow rate of 275 mL·min^{-1} could basically overcome gas diffusion resistance, and further increase in H_2 flow rate is unnecessary.

The effect of H_2 flow rate on polarization curve with nickel particle content of 7.89% in the anode is shown in Fig. 5. The H_2 flow rates here are also selected as 75, 140, 275 and 385 mL·min^{-1}. Polarization performance of the anode is promoted evidently as the H_2 flow rate increases before 275 mL·min^{-1}, in terms of increase in both limiting current density and current density under the same overpotential. Increase of gas velocity enhances random motion of nickel particles and the enhanced random motion of particles reduces diffusion layer thickness, resulting in a higher mass transfer coefficient. Therefore, concentration polarization is reduced for the promoted transfer of reactant from environment to electrode surface and transfer of product from electrode surface to environment. In addition, a higher H_2 flow rate also means higher concentration of reactant in molten carbonate, which accelerates the anodic reaction (Eq. (2)) to the positive direction. And that produces more free electrons, which means a higher current density. However, when H_2 flow rate exceeds 385 mL·min^{-1}, excess high flow rate may deteriorate the contact between nickel particles as well as the contact between nickel particles and the current collector. Therefore, the ohmic polarization is increased, which leads to a decrease in polarization performance.

2. The Influence of Nickel Particle Content

The nickel particle content is defined as follows:

$$\text{Nickel particle content} = \frac{\text{Weight of nickel particles}}{\text{Weight of nickel particles} + \text{Weight of carbonate}} \quad (3)$$

With the use of a cylindrically curved nickel plate current collector, H_2 flow rate of 275 mL·min^{-1}, reaction temperature of 923 K, O_2/CO_2 flow rate of 10/20 mL·min^{-1} and O_2/CO_2 ratio of 1 : 2, Fig. 6 shows the influence of nickel particle content on polarization performance. The anode polarization performance is promoted stably as nickel particle content increases. However, when nickel particle content exceeds 7.89%, both limiting current density and current density under the same overpotential decrease. The limiting current density with nickel particle content of 7.89% is nearly twice as much as that without nickel particles in the anode. The activity of H_2 in molten carbonate (Eq. (2)) is low to some extent, while the reaction could easily occur under nickel catalyst. Therefore, a higher nickel particle content increases the catalyst surface area, which is helpful to enhance the contact area among the gaseous phase, liquid phase and solid phase, resulting in more free electrons. Meanwhile, the increase in nickel particle content also favors the contact probability between the nickel particles and the current collector and promotes the efficiency of current collection, which leads to a relatively large current density. Nevertheless, an exorbitant nickel particle content may cause deterioration of fluidization in the anode,

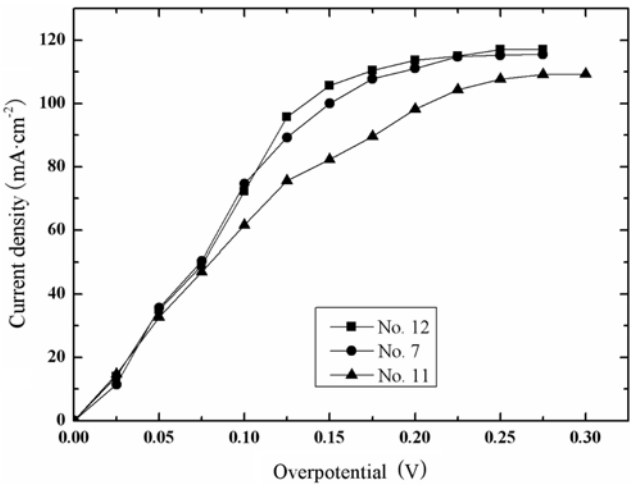

Fig. 7. Polarization curves for anode at different O_2/CO_2 flow rates.

which degrades the contact between the nickel particles and the current collector. As a result, the degradation in the polarization performance of anode is observed despite a big surface area of catalyst.

3. The Influence of O_2/CO_2 Flow Rate

Fig. 7 shows how O_2/CO_2 flow rate affects polarization curves. With the O_2 flow rate varying as 5, 10 and 15 mL·min^{-1}, the limiting current density of anode reaches 109.3, 115.6 and 117.0 mA·cm^{-2} respectively. An increase in O_2/CO_2 flow rate promotes anode polarization performance, especially when it is lower than 10/20 mL·min^{-1}. The increased flow rate of O_2/CO_2 enhances the dissolved amount of the O_2 and CO_2 in molten carbonate, and the enhanced dissolved amount of reactant would accelerate anodic reactions. In addition, increase in gas flow rate would strengthen mass transfer in reference electrode, which reduces its concentration polarization. However, the polarization curve stays steady after O_2/CO_2 flow rate reaches 10/20 mL·min^{-1}. It is probably due to the O_2 as well as CO_2 in molten carbonate having reached saturated and the flow rates having been able to reduce the concentration polarization well. Therefore, a further increase in the gas flow rate shows little effect on the polarization curves.

4. The Influence of Reaction Temperature

The effect of reaction temperature on the polarization curve is presented in Fig. 8. The reaction temperatures selected for the experiment are 873, 898, 923 and 948 K, and the limiting current density of FBEFC anode is 82.0, 104.0, 115.6 and 130.3 mA·cm^{-2}, respectively. Meanwhile, a gradual increase in current density under the same overpotential is also observed. Higher temperature reduces the activation energy barrier of H_2, which makes the anode electrochemical reaction become easier. It is well known that more anodic reactions produce more free electrons and more free electrons bring larger current density. In addition, a higher reaction temperature also increases the conductivity of carbonate ion, which results in low ohmic polarization. However, oxidization in the oxidizing atmosphere and corrosion in molten carbonate are aggravated at high temperature. Therefore, an extremely high temperature (higher than 923 K) is not suggested for the sake of the experimental device's protection.

5. The Influence of Current Collector Type

With H_2 flow rate of 275 mL·min^{-1}, reaction temperature of 923 K, O_2/CO_2 flow rate of 10/20 mL·min^{-1}, O_2/CO_2 ratio of 1 : 2 and nickel particle content of 7.89%, the effect of current collector type on the polarization curve is presented in Fig. 9. It is obvious that the polarization performance of the anode with a cylindrically curved nickel plate current collector is better than that with a flat nickel plate current collector, and the limiting current density of the former is 20% higher than that of the latter. The cylindrically curved nickel plate current collector has a larger area than the flat nickel plate current collector, which facilitates the contact between nickel particles and current collector. In addition, the working electrode includes nickel particles and current collector in our experiment and the use of cylindrically curved nickel plate current collector enlarges the working electrode surface area. These give a larger anode current density with a cylindrically curved nickel plate current collector than that with a flat nickel plate current collector.

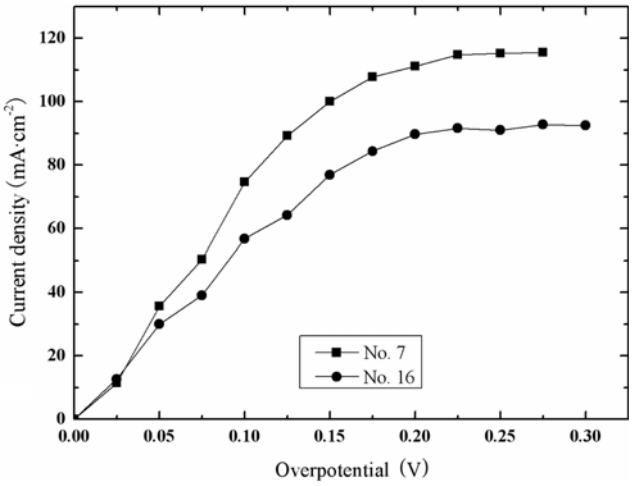

Fig. 9. Polarization curves for anode with different current collectors.

6. The Influence of O_2/CO_2 Ratio

The effect of the O_2/CO_2 ratio (1 : 3, 1 : 2 and 1 : 1) on the polarization curve is demonstrated in Fig. 10. The optimum O_2/CO_2 ratio of 1 : 2 could be easily obtained from the figure. And both the increase and decrease of the ratio degrade the fuel cell performance.

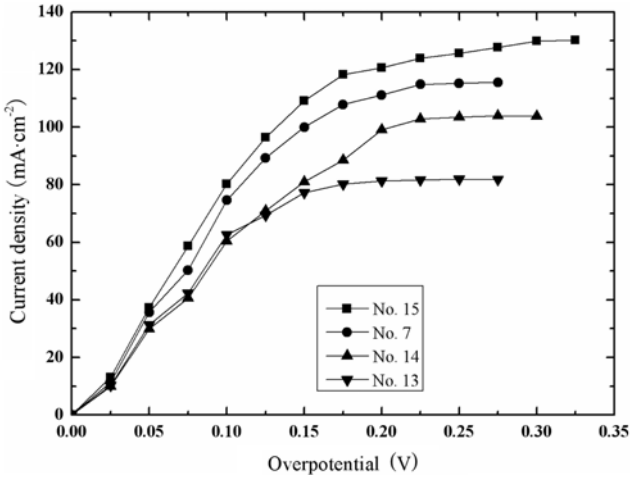

Fig. 8. Polarization curves for anode at different reaction temperatures.

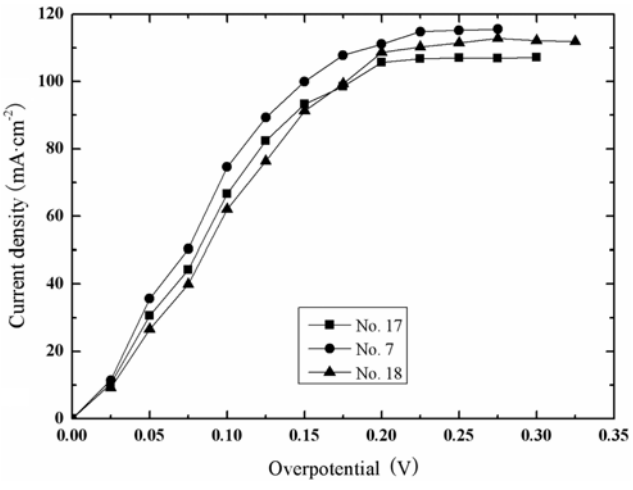

Fig. 10. Polarization curves for anode at different O_2/CO_2 ratios.

This ratio is also the optimum one in the MCFC which shares the same cathodic reaction with FEBFC (Eq. (4)). Besides, the O_2/CO_2 ratio of 1 : 2 was adopted in Matsuno's research, giving a relative predominant performance in the fuel cell. However, how the changes in O_2 and CO_2 ratios affect the polarization curve needs to be further investigated in future work.

$$O_2+2CO_2+4e^-=2CO_3^{2-} \quad (4)$$

CONCLUSIONS

The polarization performance of an FBEFC anode was investigated. The increase in H_2 flow rate gradually promoted anode polarization performance. However, when the H_2 flow rate exceeded 275 $mL\cdot min^{-1}$, the promotion in performance of anode without nickel particles was no longer evident, while the anode performance with nickel particle content of 7.89% degraded. Increase in nickel particle content enhanced the current density. Nevertheless, an excess of nickel particles would induce agglomeration in the bed and lead to low limiting current density. Increase in O_2/CO_2 flow rate promoted anode performance. But the effect was inconspicuous when the flow rate was over 10/20 $mL\cdot min^{-1}$. The O_2/CO_2 ratio of 1 : 2 gave a bigger limiting current density than other ratios. Limiting current density and current density under the same overpotential were increased all the times with the increase in reaction temperature. The anode with cylindrically curved nickel plate current collector showed larger current density than that with flat nickel plate current collector.

ACKNOWLEDGEMENTS

We gratefully acknowledge the support of the National Natural Science Fund Program of China (50776019), the Doctoral Subject Science &Technology Fund Program of State Education Ministry of China (200802860038) and the Science & Technology Foundation of Southeast University of China (XJ0703267).

REFERENCES

1. M. Bischoff and G. Huppmann, *J. Power Sources*, **105**, 216 (2002).
2. A. L. Dicks, *Curr. Opin. Solid State Mater. Sci.*, **8**, 379 (2004).
3. S. A. Hong, T. H. Lim, S. W. Nam, I. H. Oh and H. C. Lim, *Korean J. Chem. Eng.*, **17**, 193 (2000).
4. S. Y. Lee, H. C. Lim and G. Y. Chung, *Korean J. Chem. Eng.*, **27**, 487 (2010).
5. R. Rashidi, I. Dincer and P. Berg, *J. Power Sources*, **185**, 1107 (2008).
6. W. He and Q. Chen, *J. Power Sources*, **73**, 182 (1998).
7. H. Morita, M. Komoda, Y. Mugikura, Y. Izaki, T. Watanabe, Y. Masuda and T. Matsuyama, *J. Power Sources*, **112**, 509 (2002).
8. Y. Matsuno, K. Suzawa, A. Tsutsumi and K. Yoshida, *Int. J. Hydrog. Energy*, **21**, 195 (1996).
9. Y. Matsuno, A. Tsutsumi and K. Yoshida, *Int. J. Hydrog. Energy*, **21**, 601 (1995).
10. Y. Matsuno, A. Tsutsumi and K. Yoshida, *Int. J. Hydrog. Energy*, **21**, 663 (1996).
11. Y. Matsuno, A. Tsutsumi and K. Yoshida, *Int. J. Hydrog. Energy*, **22**, 615 (1997).
12. S. C. Yen and C. Y. Yao, *J. Electrochem. Soc.*, **138**, 2344 (1991).
13. N. Vatistas and M. Bartolozzi, *J. Appl. Electrochem.*, **20**, 951 (1990).
14. C. Y. Yap and N. Mohamed, *Chemosphere*, **67**, 1502 (2007).
15. K. Kusakabe, S. Morooka and Y. Kato, *J. Chem. Eng. Jpn.*, **14**, 208 (1981).
16. X. Hu and R. G. Bautista, *Sep. Sci. Technol.*, **32**, 1769 (1997).
17. S. Li, A. C. Lee, R. E. Mitchell and T. M. Gur, *Solid State Ionics*, **179**, 1549 (2008).
18. T. Berent, R. Mason and I. Fells, *J. Appl. Chem. Biotechnol.*, **21**, 71 (1971).